

# Highly coherent thermal emission obtained by plasmonic bandgap structures

Gabriel Biener, Nir Dahan, Avi Niv, Vladimir Kleiner, and Erez Hasman<sup>a)</sup>

Micro and Nanoptics Laboratory, Faculty of Mechanical Engineering and Russel Berrie Nanotechnology Institute, Technion-Israel Institute of Technology, Haifa 32000, Israel

(Received 5 August 2007; accepted 21 January 2008; published online 27 February 2008)

We demonstrate an extraordinary quasimonochromatic thermal emission with high spatial coherence length ( $l_c > 2400\lambda$ ) and a quality factor  $Q=2320$  at radiation frequencies that are much smaller than the plasma frequency of metal ( $\omega \ll \omega_p$ ). This emission is achieved by forming a plasmonic bandgap, which is obtained by a periodic structure on a metallic surface. Such a structure modifies the dynamics of the surface wave and results in a van Hove singularity [Van Hove, Phys. Rev. **89**, 1189 (1953)] in the spectral density of states while maintaining a large coherence length. © 2008 American Institute of Physics. [DOI: 10.1063/1.2883948]

Thermal sources are often considered to be isotropic and incoherent. Nevertheless, highly directional quasimonochromatic infrared (IR) thermal radiation has been demonstrated in the last few years.<sup>1-6</sup> Such a radiation is achieved by forming a cavity using one- or two-dimensional photonic crystal structures.<sup>1,2</sup> Another method exploits surface waves, such as surface phonon polariton, supported by polar materials, and surface plasmon polariton (SPP), supported by metals. The coupling of such waves to radiative beams is achieved using a periodic structure that is embedded in a surface of a polar or a metallic material.<sup>3-6</sup> In the case of a shallow structure, i.e.,  $\xi \equiv h/d_s \leq 1$  ( $h$  is the structure thickness and  $d_s$  is the skin depth inside the material), the radiative field is dominated by the behavior of the delocalized surface wave. Thus, the coherence length of the radiative field,  $l_c$ , is limited by that of the delocalized surface wave,  $L_c \cong \pi/[2 \text{Im}(k_{\text{SPP}})]$ , with the wavenumber  $k_{\text{SPP}} = (\omega/c) \sqrt{\epsilon_m \epsilon_d / (\epsilon_m + \epsilon_d)}$ , ( $\epsilon_m$  and  $\epsilon_d$  are the material's and the surrounding dielectric constants, respectively).<sup>5</sup> Additionally, the thermal radiation of the coupled radiative field is affected by the density of states (DOS) of the delocalized surface wave  $\rho_{\text{SPP}} \propto 1/v_g$ , where  $v_g = d\omega/dk_{\text{SPP}}$  is the group velocity. Close to the surface wave's resonance frequency ( $\omega \approx \omega_p/\sqrt{1+\epsilon_d}$ ,  $\omega_p$  is the plasma frequency), the field is characterized by a high DOS ( $v_g \rightarrow 0$ ) and a relatively low coherence length (typically,  $L_c = 50\lambda$  where  $\lambda$  is the wavelength). Conversely, in the low frequency region,  $\omega \ll \omega_p$ , the surface wave is characterized by a low DOS ( $v_g \rightarrow c$ ) and a high coherence length (typically,  $L_c = 10^3\lambda$  in metals). In this region, the surface wave exhibits photonlike behavior [see the inset of Fig. 1(a)]. Surface waves have been exploited to enhance thermal emission close to their resonance frequency, for instance, SPPs on a gold surface in the visible region or surface phonon polaritons on SiC in the IR.<sup>5,7</sup> The coherence length of the experimentally demonstrated emissions was on the order of  $l_c = 50\lambda$ . Accordingly, by exploiting the surface wave in the photonlike region, we can achieve a coherence length with an order of magnitude larger than the one demonstrated above, but with a low DOS. This behavior can be expected from metals which have a plasma frequency, typically, in the ultraviolet range, while the thermal emission is considered in

the mid-IR region. Note that it is possible to tailor the plasma frequency by using a subwavelength periodic structure embedded in a metal substrate.<sup>8</sup> Unfortunately, this method is not adequate for achieving thermal emissions with a high coherence length, since the emission spectrum is near the modified SPP resonance frequency. Consequently, we pose the question: Is it possible to exploit the high coherency of the surface wave in the photonlike region by coupling it to a radiative field while enlarging the DOS?

In this letter, we propose forming a plasmonic bandgap<sup>9-12</sup> that is realized by a periodic structure on a metallic surface. The proposed structure is thicker than the skin depth,  $\xi \sim 10$ , and thus modifies the dynamics of the surface wave. As a result, the reciprocal relationships imposed by the delocalized surface wave between the DOS and the coherence length no longer apply. With this mechanism, we sig-

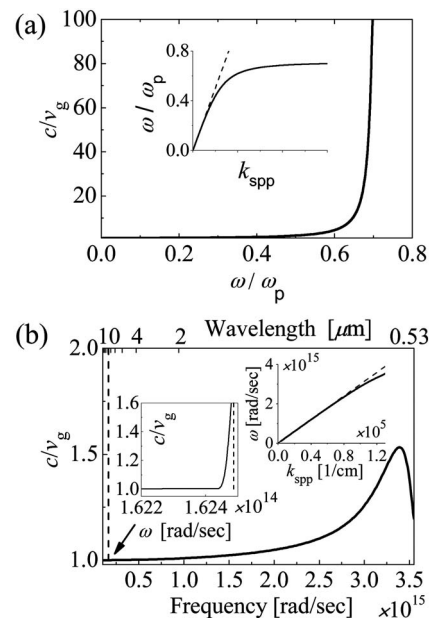


FIG. 1. (a)  $c/v_g$  of delocalized SPPs vs frequency for (a) lossless metal and (b) gold. The singularity near  $11.6 \mu\text{m}$  wavelength due to the plasmonic bandgap structure [derived from Fig. 2(d)] is also shown. The insets depict the dispersion curves of the delocalized SPPs within the metallic substrate/air interface where the dashed line denotes the light line. A magnified area of the van Hove singularity in plasmonic bandgap structure is shown in the inset near  $10 \mu\text{m}$  wavelength.

<sup>a)</sup>Electronic mail: mehasman@tx.technion.ac.il.

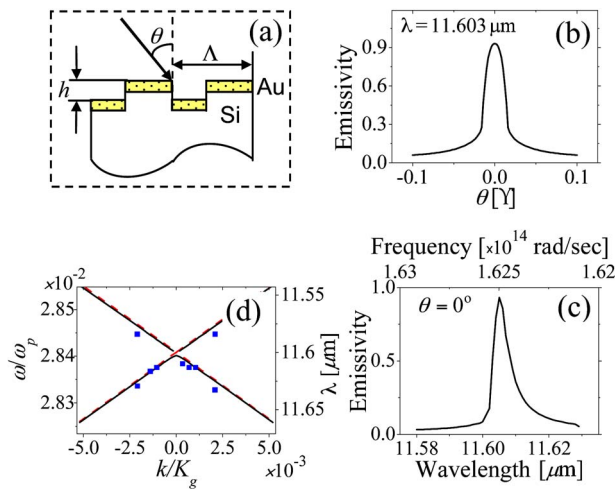


FIG. 2. (Color online) (a) Schematic representation of the metallic grating. Calculated emissivity of a metallic gold grating, with period  $\Lambda=11.6 \mu\text{m}$ , fill factor  $q=0.47$ , and  $\xi=8.4$ , as a function of (b) observation angle and (c) wavelength. (d) Experimental (squares) and calculated (solid line) dispersion curves of the metallic grating ( $K_g=2\pi/\Lambda$ ). Dashed red line indicates the Rayleigh anomaly.

nificantly enlarge the DOS of the surface wave ( $1/v_g \rightarrow \infty$ ) near the bandgap, and as a consequence, we enlarge the emissivity of the radiative field as well. In the case of a small photonic bandgap (PBG), the large coherence length, which is inversely proportional to the gap size ( $L_c \propto d^2 \omega / dk^2 \propto 1/\text{PBG}$ ), is maintained.<sup>10</sup> The analysis of the proposed periodic structure on a gold surface yielded a thermal emission with a spatial coherence length  $l_c > 2400\lambda$  and a quality factor  $Q=2320$  (where  $Q=\lambda/\Delta\lambda$ ) around  $11.6 \mu\text{m}$  wavelength. This coherence length is more than an order of magnitude larger than the highest coherence length reported to date. The measured coherence length, which was limited by the element dimensions, resulted in  $l_c=862\lambda$  (angular divergence of  $0.066^\circ$ ) and with the quality factor  $Q=460$ . This result confirms the ability to obtain high emission with large spatial and temporal coherence.

It is well known that metals support SPPs in the frequency region for which the real part of the dielectric constant is smaller than  $-1$ .<sup>5</sup> This region includes frequencies that are lower than the resonance frequency of the surface wave within the metal air interface,  $\omega_p/\sqrt{2}$ . Figure 1 depicts  $c/v_g$  of the delocalized SPPs versus the frequency, derived from the dispersion curve (in the inset), for a lossless metal [Fig. 1(a)] and for real gold [Fig. 1(b)]. The dielectric constant of the gold was taken from Ref. 13. An increase of the DOS is discerned near the resonant frequency (visible region). A periodic structure on the metal substrate can produce singularities in the DOS (singularity in  $1/v_g$ ). These critical points in the spectrum are known as the van Hove singularities.<sup>14</sup> We find a strong effect of these singular points, due to plasmonic bandgap structure, on the thermal emission of gold in the mid-IR region. As an example, we have calculated the emissivity of a gold grating with a period of  $\Lambda=11.6 \mu\text{m}$ , fill factor  $q=0.47$ , and  $\xi=8.4$  (i.e., a thickness of  $270 \text{ nm}$  with a skin depth of  $32 \text{ nm}$ ) by using a rigorous coupled wave analysis. Figure 2(a) is a schematic representation of the calculated grating. Figures 2(b) and 2(c) depict the calculated emissivity as a function of the observation angle and the wavelength, respectively. Such a structure results in a high emissivity with an extraordinary spatial co-

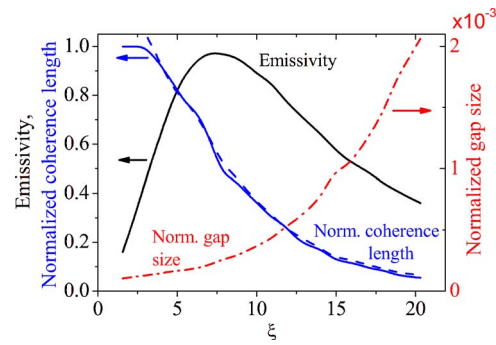


FIG. 3. (Color online) Calculated emissivity (black line), normalized gap size  $\text{PBG}/\omega$  (dashed dotted red line), and normalized coherence length  $l_c/L_c$  (blue line) as a function of  $\xi$ , ( $\xi=h/d_s$ ). The gap is normalized to the emission frequency and the coherence length is normalized to the delocalized surface wave coherence length. Blue dashed line is calculated as  $\alpha/\text{PBG}$ , where  $\alpha$  is the proportionality constant and  $\text{PBG}$  is the photonic bandgap size.

herence  $l_c=\lambda/\Delta\theta=2414\lambda$ , and a temporal coherence indicated by the quality factor  $Q=2320$ .

To understand the behavior of such a structure, we make use of the dispersion curve, as depicted in Fig. 2(d). When magnifying the central region of the first Brillouin zone in the vicinity of the emitted frequency, a small gap appears. This small gap indicates that a high DOS exists at the frequency's vicinity of the gap,<sup>9–12</sup> along with high coherence resulting from the small gap size.<sup>10</sup> Figure 3 depicts the calculated bandgap and coherence length as a function of the grating depth  $\xi$ . The reciprocal relation between the gap size and the coherence length is evident. As can be seen in this figure, at the region of  $\xi=1$ , the coherence length of the radiative field is dominated by the delocalized surface wave. Figure 3 also depicts the emissivity of the grating versus  $\xi$ . High emissivity is observed between  $\xi=5$  and  $10$ , in which the coherence length is considered to be large.

We realized the calculated grating on a Si substrate using photolithographic and etching processes. The grating, which is  $10 \text{ mm}$  in diameter, had a  $150 \text{ nm}$  gold layer deposited on it. Figure 4(a) shows an atomic force microscope image of the

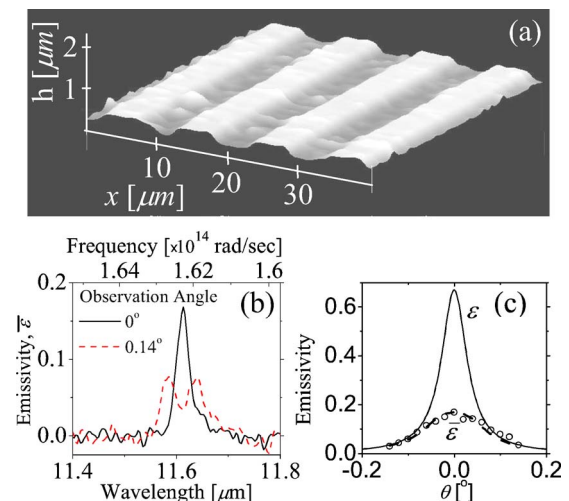


FIG. 4. (Color online) (a) Atomic force microscope image of the realized grating, (b) measured emissivity as a function of the wavelength for  $\theta=0^\circ$  and  $0.14^\circ$ , and (c) emissivity (solid line) vs observation angle, as extracted from the measured emissivity (open circles). The dashed line indicates an integrated emissivity obtained by a convolution analysis between the emissivity and a simulated slit of  $\Delta\theta=0.1^\circ$ .

the realized grating. Subsequently, we measured the emission using a Fourier transform IR spectrometer (Bruker-vertex 70) while heating the structure to 403 K. Figure 4(b) depicts the measured emissivity as a function of the wavelength. The measured emissivity  $\bar{\epsilon}$  is actually the integrated emission from the grating over a slit of  $\Delta\theta=0.1^\circ$  normalized by the blackbody emission from the same slit. As can be seen,  $\bar{\epsilon}$  is quasimonochromatic with  $Q \approx 460$  ( $\Delta\lambda=25$  nm). Figure 4(c) depicts the emissivity  $\epsilon$  (solid line) versus the observation angle, as was extracted from  $\bar{\epsilon}(\theta)$ , where  $\bar{\epsilon}(\theta)$  is a convolution between the emissivity and a slit of  $\Delta\theta=0.1^\circ$ . As can be seen, the emissivity is high along with high measured coherence length, which equals  $862\lambda$ . We would like to note that this coherence length is equal to the element size of 10 mm, thus indicating the lower limit for the actual coherence length. As part of the analysis of the small plasmonic bandgap, we plotted the experimental dispersion curve onto the theoretical curve and found the values to be in close agreement [see Fig. 2(d)]. The difference between the experimental and the theoretical results is due to the slight imperfections in the fabricated grating, as well as the dependence of the gold refractive index on the temperature. The  $1/v_g(\omega)$  near the bandgap derived from the dispersion curve [see Fig. 1(b)] confirms the appearance of a singularity due to a plasmonic bandgap.

To conclude, we have demonstrated an extraordinary thermal emission with a large spatial and temporal coherence from a metallic grating in the mid-IR radiation frequency which is much smaller than the plasma frequency of the metal. As demonstrated in this letter, we have overcome the low DOS problem of the delocalized surface wave by forming a plasmonic bandgap structure near the emitted wavelength. The analyzed structure's thickness is greater than the

skin depth ( $\xi \sim 10$ ). This structure affects the SPP dynamics and provides us with the opportunity to engineer the dispersion relation, i.e., enlarge the DOS while maintaining the large coherence length, by imposing a small gap. Another advantage for choosing metal as a thermal source concerns the large bandwidth in which SPPs are supported. By exploiting the plasmonic bandgap structure method, we can tailor the gap around any required frequency within the supporting spectrum and thus tune the emission frequency.

<sup>1</sup>I. Celanovic, D. Perreault, and J. Kassakian, *Phys. Rev. B* **72**, 075127 (2005).

<sup>2</sup>I. Puscasu, M. Pralle, M. McNeal, J. Daly, A. Greenwald, E. Johnson, R. Biswas, and C. G. Ding, *J. Appl. Phys.* **98**, 013531 (2005).

<sup>3</sup>N. Dahan, A. Niv, G. Biener, V. Kleiner, and E. Hasman, *Appl. Phys. Lett.* **86**, 191102 (2005).

<sup>4</sup>M. Laroche, C. Arnold, F. Marquier, R. Carminati, J.-J. Greffet, S. Collin, N. Bardou, and J. L. Pelouard, *Opt. Lett.* **30**, 2623 (2005).

<sup>5</sup>K. Joulain, J. P. Mulet, F. Marquier, R. Carminati, and J.-J. Greffet, *Surf. Sci. Rep.* **57**, 59 (2005).

<sup>6</sup>N. Dahan, A. Niv, G. Biener, Y. Gorodetski, V. Kleiner, and E. Hasman, *Phys. Rev. B* **76**, 045427 (2007).

<sup>7</sup>M. Kreiter, J. Oster, R. Sambles, S. Herminghaus, S. Mittler-Neher, and W. Knoll, *Opt. Commun.* **168**, 117 (1999).

<sup>8</sup>J. B. Pendry, L. Martin-Moreno, and F. J. Garcia-Vidal, *Science* **305**, 847 (2004).

<sup>9</sup>E. Yablonovitch, *Phys. Rev. Lett.* **58**, 2059 (1987).

<sup>10</sup>H. Rigneault, J. M. Lourtioz, C. Delalande, and A. Levenson, *Nanophotonics* (ISTE, London, 2006).

<sup>11</sup>A. Christ, T. Zentgraf, J. Kuhl, S. G. Tikhodeev, N. A. Gippius, and H. Giessen, *Phys. Rev. B* **70**, 125113 (2004).

<sup>12</sup>S. C. Kitson, W. L. Barnes, and J. R. Sambles, *Phys. Rev. Lett.* **77**, 2670 (1996).

<sup>13</sup>P. G. Etchegoin, E. C. Le Ru, and M. Meyer, *J. Chem. Phys.* **125**, 164705 (2006).

<sup>14</sup>L. Van Hove, *Phys. Rev.* **89**, 1189 (1953).